http://dx.doi.org/10.5012/bkcs.2013.34.8.2519

Platinum Nanoparticles Supported on Exfoliated Layered Double Hydroxides Nanosheet as a Reusable Catalyst for the Reduction of 4-Nitrophenol

Jungwoon Na, Jiwon Moon, Hye Ran Cho, Jiye Hwang, and Jong Hyeon Lee*

Department of Chemistry, The Catholic University of Korea, Bucheon, Gyeonggi 420-743, Korea
**E-mail: jhlee305@catholic.ac.kr*
Received April 8, 2013, Accepted May 10, 2013

Key Words : Platinum nanoparticle, Layered double hydroxide nanosheet, Nanocomposite

Supported transition metal nanoparticles (NPs) have attracted much interest in the field of heterogeneous catalysts,[1] because the nature of supporting materials offers a strong possibility of controlling metal particle size and preventing the aggregation of metal NPs, which can consequently affect the catalytic performance of the supported NPs.[2] Mesoporous silica,[3] graphitic carbons,[4] polymer nanobeads[5] and layered double hydroxides (LDHs)[6] have been potentially used as the supports to immobilize the metal NPs. Recently, two-dimensional nanosheets of exfoliated LDHs[7] have emerged as a new type of supports to immobilize the metal NPs due to the unique two dimensional structure and large reactive surface of the LDH host layers. However, there have been only a few papers reported on the synthesis of metal NPs in the exfoliated LDH nanosheets. The LDHs, also known as hydrotalcite-like clays, consist of positively charged metal hydroxides and charge balancing anions, expressed by the general formula $[M^{2+}_{(1-x)}M^{3+}_{x}(OH)_2]A^{n-}_{x/n}\cdot mH_2O$, wherein M^{2+} and M^{3+} can be any divalent and trivalent metal cation occupied in the octahedral holes of a brucite-like layer and A^{n-} is any hydrated exchangeable anion positioned in the gallery between the layers through a strong electrostatic and intermolecular interaction.[8]

The LDH nanosheets with a high-level of positive charge density can be produced by the exfoliation of LDHs into single hydroxide layers, which leads to electrostatic interactions between the LDH layers and metal precursors and/or metal NPs. Recently, Haraguchi *et al.* reported Au NPs modified LDH nanosheets, prepared by *in situ* reduction of metal precursor in aqueous solution.[9] However, the aqueous media usually cause not only the LDH nanosheets to be restacked but also the metal NPs to be aggregated into large forms. We chose formamide as a reaction medium in order to exfoliate the LDHs and form the metal NPs. In this study, we present a very simple but successful synthesis of well-defined spherical Pt NPs on the LDH nanosheets without any stabilizing agent for metal NPs. We have also evaluated the catalytic performance of the Pt NP-LDH nanocomposites, prepared in this study, in the reduction of 4-nitrophenol.

The structure and synthetic procedure for the nanocomposite of the LDH nanosheet and Pt NPs in formamide are schematically described in Scheme 1. For obtaining the well-defined LDH nanosheet, as-prepared carbonate form of LDHs was hydrothermally treated and further reacted by anion-exchange with nitrate. The carbonate form of Mg_2Al-LDH crystal, which has a well-crystallized rhombohedral phase with a basal spacing of 7.56 Å, was converted into a nitrate form with an 8.96 Å basal spacing (Figure S1a) using a salt/acetate buffer treatment.[10] A characteristic band for the N-O stretching mode in the FT-IR spectra (Figure S1b) supports the intercalation of the nitrate into interlayers of the LDH crystals. The LDH crystals was exfoliated in formamide by continuous stirring for 5 days, and a transparent solution was then obtained as shown in Figure 1(a), indicating a successful exfoliation of the LDH crystals.[11] The solution of the exfoliated LDH nanosheets has an excellent stability for 2 months. The transmission electron microscope (TEM) image shown in Figure 1(b) clearly indicates the exfoliated LDH nanosheets maintaining their plate-like structure, with a diameter of approximately 300-400 nm. The TEM also confirms the formation of very thin nanosheets compared to the pristine LDH particle (inset in Figure 1(b)). The zeta potential measurement clearly demonstrates the positively charged state of the Mg_2Al-LDH nanosheet

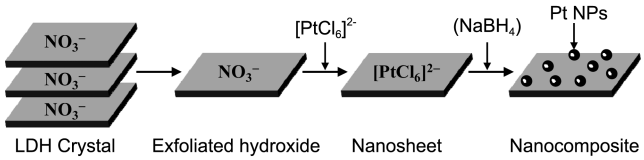

Scheme 1. Schematic representation of synthesis of Pt NPs on the exfoliated Mg_2Al-LDH nanosheet.

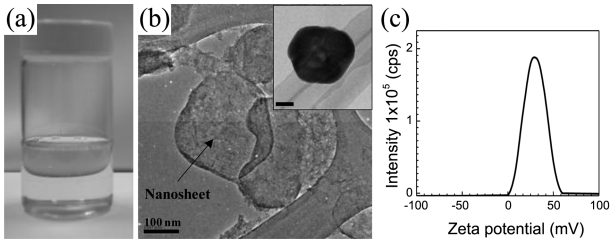

Figure 1. (a) Photograph of the Mg_2Al-LDH nanosheet suspension and (b) TEM image and (c) zeta surface potential of the Mg_2Al-LDH nanosheet. Inset in (b) shows TEM image of LDH particle.

with +29.0 mV (Figure 1(c)).

For loading Pt onto the LDH nanosheet, 90 mL of 0.1 M H_2PtCl_6 in methanol was introduced into a 10 mL solution of the LDH nanosheet with a Pt/LDH ration of 0.36 wt %, and the solution was agitated for 1 h by vigorous stirring. At this step, the $[PtCl_6]^{2-}$ ions could be electrostatically stabilized on the positively charged LDH surfaces, which was confirmed by the decreased zeta potential to +12.6 mV (Figure S2). Subsequently, 0.2 mmol of $NaBH_4$ as a reducing agent was added into the solution then agitated for 6 h with a continuous stirring. After the reaction completed, homogeneous and transparent black-brown solution was obtained as shown in the inset in Figure 2(a). The characteristic color of the solution clearly indicates the formation of Pt particles. The sample showed negative zeta potential with −3.84 mV (Figure S2), indicating the electrostatically assembled Pt NPs on the positively charged LDH nanosheets. Notably, the colloidal solution of Pt NPs was stable for a month without significant precipitation of the Pt NPs, demonstrating that all Pt NPs were successfully synthesized on the hydroxide surface of the LDH nanosheet. In the absence of LDHs, the reaction was comparatively slow and Pt particles were gradually precipitated because of a large agglomeration of unsupported Pt particles. Figure 2 collected high resolution TEM images of the Pt NP-LDH nanocomposite. Figure 2(a) shows that the exfoliated LDH nanosheet maintained its plate-like morphology and lateral dimensions after the formation of the Pt NPs. The enlarged image in Figure 2(b) clearly shows the formation of the spherical Pt NPs on the surface of the LDH nanosheet. Figure 2(c) indicates the crystalline Pt NPs with a spacing of 2.4 Å, corresponding to Pt (*111*). The TEM inspections also indicated no significant particle aggregation throughout the surface of the LDH nanosheet. The TEM results revealed that the positively charged LDH nanosheet effectively provided the formation of Pt NPs and induced the strong interaction between the LDH layers and the Pt NPs.

The catalytic activity of the Pt NPs (Figure S3) and the Pt NP-LDH nanocomposites was evaluated in the reduction of 4-nitrophenol (0.1 mM) by $NaBH_4$ (60 μmol) in the presence of the Pt NPs and the Pt NP-LDH nanocomposite solution (100 μL), respectively. The Pt content in 100 μL of Pt NP-LDH was 474 ppb. Prior to the catalytic measurements, the nanocomposite was collected by centrifugation (10,000 rpm for 10 min) and washed with ethanol several times to remove residual formamide, then dispersed into 1 mL of water. UV/Vis spectra of the reaction mixture were acquired at 2 min intervals in the range of 250-500 nm immediately after the addition of the Pt NP-LDH nanocomposites. As shown in Figure 3(a), the strong absorbance peak of 4-nitrophenolate[12] at 400 nm successfully decreased with increasing the reaction time. Simultaneously, a new peak with increased absorbance around 300 nm indicates the formation of the product 4-aminophenol.[12] The conversion efficiency was 92% in 30 min of reaction time. To evaluate the reuse performance of the catalyst, the nanocomposites were re-collected by simple centrifugation treatment (inset in Figure 3(b)) and re-dispersed into a fresh 4-nitrophenol solution. As shown in Figure 3(b), the Pt NP-LDH nanocomposites showed similar catalytic performance without significant reduction of conversion efficiencies for the same reaction time even after five running cycles. This is related to the no significant loss of the tightly assembled Pt NPs on the LDH nanosheets during the recycling of catalysts as shown in Figure S4.

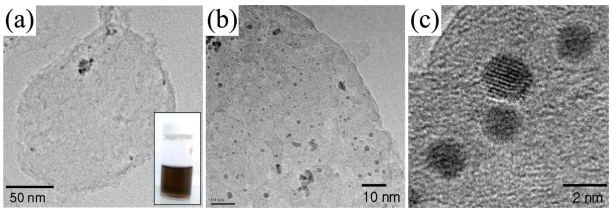

Figure 2. (a) TEM image and (b, c) HRTEM images of Pt NP-LDH nanocomposite. Inset in (a) indicates the solution of Pt NP-LDH composite.

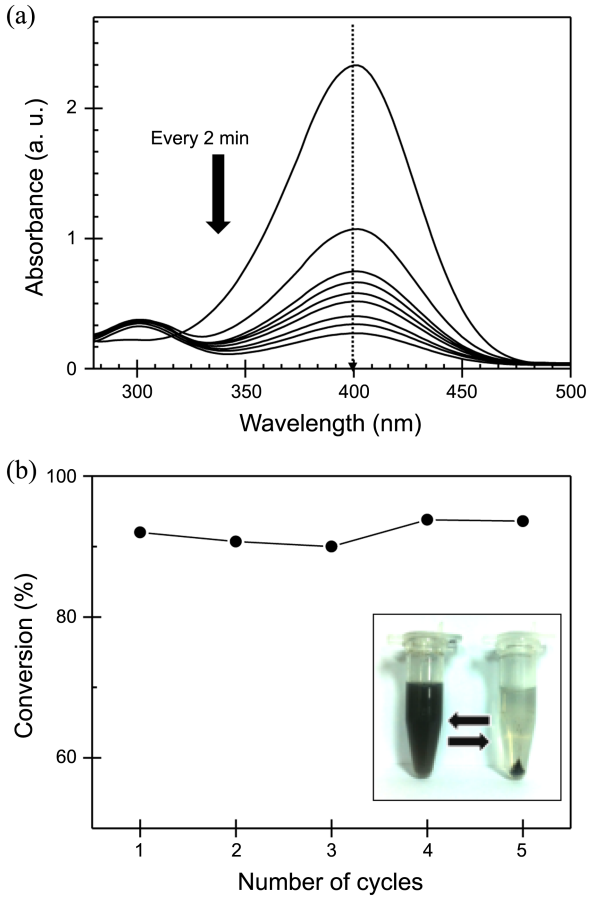

Figure 3. (a) Temporal evolution UV/Vis spectra and (b) reusability of the Pt NP-LDH nanocomposites as heterogeneous catalyst for the reduction of 4-nitrophenol in the presence of $NaBH_4$.

In summary, the well-defined spherical Pt NPs have been synthesized on the exfoliated LDH nanosheets by *in situ* reduction of H_2PtCl_6 in the formamide. The positively charged LDH nanosheet could effectively provide the formation of Pt NPs on the nanosheet and induce the strong

interaction between the LDH layer and the Pt NPs. The Pt NP-LDH nanocomposite exhibited an excellent reusability in the reduction of 4-nitrophenol due to the tightly assembled Pt NPs on the LDH nanosheets during the recycling reactions. The utilization of the double hydroxide nanosheet as a new type of supports for transition metal NPs will dramatically improve the durability in heterogeneous catalysts.

Experimental

Synthesis of Pt NPs on Exfoliated LDH Nanosheet. Mg_2Al-LDH powder (Mg/Al = 2) in carbonate form was synthesized by coprecipitation,[13] then hydrothermally treated to improve its crystallinity.[14] Following anion-exchange reaction with sodium nitrate in a salt/acetate buffer, a nitrate form of Mg_2Al-LDH was produced.[10] The LDH-nitrate sample was dried at less than 10^{-2} Torr for 24 h, then exfoliated in formamide by continuous stirring for 5 days. Weight concentration of the exfoliated LDH nanosheet was 1 mg/mL. Pt NPs on LDH nanosheet was prepared by *in-situ* chemical reduction method of H_2PtCl_6 (409.82 g/mol, Alfa Aesar) with $NaBH_4$. The product was washed with ethanol three times by centrifugation (10,000 rpm, 10 min) and finally redispersed into 1 mL of de-ionized water.

Characterizations. HRTEM images were taken using a JEM-3010 (JEOL). UV/Vis spectra were measured using a Lambda 1050 (Perkin Elmer). X-Ray diffraction (XRD) data were collected on a Siemens D5000 diffractometer with CuKα radiation at $\lambda = 1.542$ Å. Fourier-transform infrared spectroscopy (FT-IR) spectra for powder were recorded on a IRAffinity-1 (Shimadzu) equipped with a diamond accessory of an attenuated total reflectance (ATR) mode within the range of 400-4000 cm^{-1} with 100 scans at 4 cm^{-1} resolution. Zeta potential was measured using a Zetasizer nano ZS (Malvern Instruments). Pt content was measured by inductively coupled plasma mass spectroscopy (ICP-MS, NexION 300X, Perkin Elmer).

Acknowledgments. This research was supported by the Basic Science Research Program through the National Research Foundation of Korea (NRF) funded by the Ministry of Education, Science and Technology (2011-0014363), and the Research Fund-2011 of the Catholic University of Korea.

Supporting Information. XRD data and FT-IR spectra for nitrate form of Mg_2Al-LDH, particle size analysis of LDH nanosheet and zeta potentials for $[PtCl_6]^{2-}$-LDH and Pt NP-LDH composites.

References

1. (a) Tillaart, J. A. A.; Kuster, B. F. M.; Marin, G. B. *Catal. Lett.* **1996**, *36*, 31. (b) Bell, A. T. *Science* **2003**, *299*, 1688. (c) Turner, M.; Golovko, V. B.; Vaughan, O. P. H.; Abdulkin, P.; Berenguer-Murcia, A.; Tikhov, M. S.; Johnson, B. F. G.; Lambert, R. M. *Nature* **2008**, *454*, 981. (d) Narayanan, R.; El-Sayed, M. A. *J. Phys. Chem. B* **2005**, *109*, 12663. (e) Bratlie, K. M.; Lee, H.; Komvopoulos, K.; Yang, P.; Somorjai, G. A. *Nano Lett.* **2007**, *7*, 3097. (f) Lee, I.; Delbecq, F.; Morales, R.; Albiter, M. A.; Zaera, F. *Nat. Mater.* **2009**, *8*, 132.
2. In *Nanoparticles and Catalysis*; Astruc, D., Ed.; Wiley: Weinheim, 2008; p 1.
3. (a) Jiang, Y.; Gao, Q. *J. Am. Chem. Soc.* **2006**, *128*, 716. (b) Aijaz, A.; Kakamkar, A.; Choi, Y. J.; Tsumori, N.; Ronnebro, E.; Autrey, T.; Shioyama, H.; Wu, Q. *J. Am. Chem. Soc.* **2012**, *134*, 13926.
4. (a) Xia, B. Y.; Wang, J. N.; Teng, S. J.; Wang, X. X. *Chem. Eur. J.* **2010**, *16*, 8268. (b) Yin, H.; Tang, H.; Wang, D.; Gao, Y.; Tang, Z. *ACS Nano* **2012**, *6*, 8288. (c) Li, H.; Han, L.; Cooper-White, J.; Kim, I. *Green Chem.* **2012**, *14*, 586.
5. Chen, C.-W.; Serizawa, T.; Akashi, M. *Chem. Mater.* **1999**, *11*, 1381.
6. (a) Choudary, B. M.; Madhi, S.; Chowdari, N. S.; Kantam, M. L.; Sreedhar, B. *J. Am. Chem. Soc.* **2002**, *124*, 14127. (b) Choudary, B. M.; Roy, M.; Roy, S.; Kantam, M. L. *J. Mol. Catal. A-Chem.* **2005**, *241*, 215. (c) Zhao, M.-Q.; Zhang, Q.; Zhang, W.; Huang, J.-Q.; Zhang, Y.; Su, D. S.; Wei, F. *J. Am. Chem. Soc.* **2010**, *132*, 14739. (d) Shi, Y.; Yang, H.; Zhao, X.; Gao, T.; Chen, J.; Zhu, W.; Yu, Y.; Hou, Z. *Catal. Commun.* **2012**, *18*, 142. (e) Zhang, F.; Zhao, X.; Feng, C.; Li, B.; Chen, T.; Lu, W.; Lie, X.; Xu, S. *ACS Catal.* **2011**, *1*, 232.
7. (a) Yan, D.; Lu, J.; Ma, J.; Wei, M.; Evans, D. G.; Duan, X. *Angew. Chem. Int. Ed.* **2011**, *50*, 720. (b) Li, L.; Feng, Y.; Li, Y.; Zhao, W.; Shi, J. *Angew. Chem. Int. Ed.* **2009**, *48*, 5888. (c) Wang, L.; Wang, D.; Dong, X. Y.; Zhang, Z. J.; Pei, X. F.; Chen, X. J.; Chen, B.; Jin, J. *Chem. Commun.* **2011**, *47*, 3556. (d) Lee, J. H.; Chang, J.; Cha, J.-H.; Jung, D.-Y.; Kim, S. S.; Kim, J. M. *Chem. Eur. J.* **2010**, *16*, 8296.
8. (a) Kahn, A. I.; O'Hare, D. *J. Mater. Chem.* **2002**, *12*, 3191. (b) Newman, S.; Jones, W. *New J. Chem.* **1998**, *22*, 105.
9. Varade, D.; Haraguchi, K. *J. Mater. Chem.* **2012**, *22*, 17649.
10. Iyi, N.; Sasaki, T. *J. Colloid. Interf. Sci.* **2008**, *322*, 237.
11. Li, L.; Ma, R.; Ebina, Y.; Iyi, N.; Sasaki, T. *Chem. Mater.* **2005**, *17*, 4386.
12. Liu, J.; Qin, G.; Reveendran, P.; Ikushima, Y. *Chem. Eur. J.* **2006**, *12*, 2131.
13. Miyata, S. *Clay. Clay. Miner.* **1975**, *23*, 369.
14. Hickey, L.; Kloprogge, J. T.; Frost, R. L. *J. Mater. Sci.* **2000**, *35*, 4347.